Printed in the Republic of Korea
ANALYTICAL SCIENCE & TECHNOLOGY
Vol. 37 No. 4, 220-229, 2024
https://doi.org/10.5806/AST.2024.37.4.220

Estimation for warfarin in pharmaceutical preparation using monolithic column

Zahraa Hadi Shareef★ and Ahmed Ali Alkarimi

Department of Chemistry, College of Science, University of Babylon, Hilla 51002, Iraq

(Received February 3, 2024; Revised March 3, 2024; Accepted April 17, 2024)

Abstract: This study aims to developing a method for estimating pharmaceutical compounds within a monolith column using high-performance liquid chromatography (HPLC). The monolithic column was prepared using copolymerization of glycidyl methacrylate, co-ethylene dimethacrylate, and co-acrylic acid inside a borosilicate tube of specific dimensions a 60 mm borosilicate tube length with 1.5 mm and 3.5 mm inner and outer diameters, respectively. A UV Ultra violet source with a wavelength of 365 nm was used, and the polymerization process involved mixing glycidyl methacrylate, acrylic acid, ethylene dimethacrylate as a binder, and 2,2-dimethoxy-2-phenyl acetate phenone as an initiator in suitable solvents consisting of ethanol and 1-hexanol. The polymerization process formed the monolith column after 4 minutes, and subsequently, the epoxy groups were altered to diol groups using 0.2 M hydrochloric acid HCl, which were pumped through the column for 3 hours at a flow rate of 10 $\mu L \cdot min^{-1}$. Various techniques, such as Scanning Electron Microscope SEM, Brunauer-Emmett-Teller BET, Fourier-transform infrared spectroscopy FT-IR and HNMR, were utilized to characterize and confirm the structure of the monolith. The prepared monolith was employed to estimate and identify the pharmaceutical compound of warfarin using high-performance liquid chromatography HPLC. The analytical curve of warfarin was linear in the range of 3 to 100 $\mu g \cdot mL^{-1}$ with an r^2 value of 0.999. The detection and quantification limits were 0.932 and 2.788 $\mu g \cdot mL^{-1}$, respectively. The molar absorptivity and Sandells sensitivity were 2.99138×10^6 $L \cdot mol^{-1} \cdot cm^{-1}$ and 103.1×10^{-3} $\mu g \cdot cm^{-2}$, respectively.

Key words: monolith, HPLC, glycidyl methacrylate, warfarin, acrylic acid

1. Introduction

Chemical separation methods play a crucial role in various fields such as chemical analysis, industrial chemistry, biomedical sciences, and synthesis.[1] Additionally, in high-productivity applications like drug discovery, there's a growing need for computational methods that yield biopharmaceutical acceptable properties from the early stages of drug development.[2] Over the past decade, porous polymer blocks have emerged as a novel class of materials, owing to their porous nature, diverse shape, and varied sizes.[3,4]

The presence of many large pores is crucial because they allow enough mobile phase to pass inside the

★ Corresponding author
Phone : +9647762775990
E-mail : zahraahadimo1983@gmail.com

monolith.it appears that polymers with macropores >50 nm effectively separate large molecules. As for the medium-sized pores, the mesopores 2–50 nm work to increase the area of the monolith surface as well as the absorptive capacity of the monolith. Regarding the small pores, the micropores 2 nm allow the solvent to travel through the monolithic column more quickly than the packed column, reducing the columns back pressure when high flow rates are applied.[5] Therefore, the main and distinctive feature of monoliths is that they possess a large surface area and a large number of small pores, which leads to an increase in the active sites of the dissolved material present in the mobile phase.[6] Hydrophilic interaction liquid chromatography HILIC has emerged as a powerful chromatographic technique for the separation and analysis of polar and hydrophilic compounds.[7] HILIC has found widespread application in various fields, such as pharmaceuticals, biomedical research, and environmental analysis.[8] Warfarin is an oral anticoagulant medication primarily used to prevent blood clot formation or treat existing blood clots. It belongs to a class of medications called vitamin K antagonists VKAs. It's molecular formula is $C_{19}H_{16}O_4$.

Warfarin is weakly acidic due to the presence of a phenolic hydroxyl group.[9] *Fig.* 1. Show the structure of warfarin.

The purpose of studying the method for estimating warfarin in pharmaceutical preparation using the monolithic column GMA-co-EDMA-co-A.AC polymer is to enhance the efficiency, accuracy, and reliability of pharmaceutical analysis. This innovative approach offers high resolution, and improved sensitivity, crucial for precise quantification of warfarin in complex pharmaceutical formulations. By leveraging the unique properties of the monolithic column polymer, such as its cost-effectiveness and compatibility with various analytical techniques, this research aims to provide a robust method for pharmaceutical quality control, ensuring compliance with regulatory standards and ultimately enhancing drug safety and efficacy.

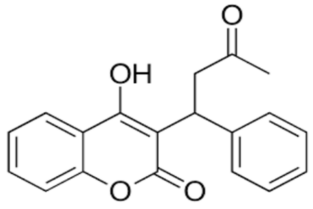

Fig. 1. Structure of warfarin.

2. Experimental

2.1. Materials

The standards used in the (HPLC) monolithic column, Glycidyl methacrylate GMA, ethylene dimethacrylate EDMA, 3-trimethoxysilyl propyl methacrylate, 2,2-dimethoxy2-phenyl acetophenone DAP, acetonitrile, and acetone were purchased from (Sigma-Aldrich), the acrylic acid, and sodium hydroxide were products of (BDH), the Hexanol, and hydrochloric acid were products of (Merck), the warfarin was product of Samarra company (Iraq), while the Formic acid and chloroform were products of (Scharlau).

2.2. Instruments of condition

The UV-Visible spectrophotometer was model UV-1700 double-beam from Shimadzu (Japan), the HPLC pump from Holliston (U.S.A), the Ultrasonic bath from (India), the syringe pump was model Bio-Analytical System Inc from (U.S.A), the irradiation device was model 220V–50 HZ from homemade (Iraq), the Fourier-transform infrared spectroscopy FT-IR was model 380 spectra Bruker from (Germany), the Scanning Electron Microscope SEM TESCAN was model Mira3 from (Czech Republic), the Brunauer-Emmett-Teller BET technique was model BELSORP MINI II from (Japan), and the Hydrogen nuclear magnetic resonance HNMR was model Oxford 500 Magnet from (U.S.A).

2.3. Sample preparation

2.3.1. Preparation of warfarin solutions

Warfarin was prepared as a standard solution with a concentration of 100 $\mu g \cdot mL^{-1}$. From this standard solution, other concentrations were prepared.

2.3.2. Preparation of sample solutions

A weight of 1 mg of warfarin flamingo tablet and

5 mg of ciplato tablet were taken and it was ground well, they were then dissolved with a suitable solvent using distilled water and placed in an ultrasonic sonication device. The resulting solution was transferred to a 100 mL glass beaker to form concentration solutions of 10 ppm and 50 ppm. The solutions were subjected to filtration.

2.3.3. Monolith column preparation Silanization process

Preparing the inner surface of the tube is the most crucial in forming the monolith within the borosilicate tube. 3-trimethoxysilyl propyl methacrylate reacts with silanol groups Si-OH on the borosilicate tubes inner wall. The process is to install the monolith on the inner wall of the tube and ensure that the polymer does not come out or dislodge when using a high pumping speed. As well as it helps prevent the shrinkage effect during the polymerization process. And avoid interactions that occur with silanol groups. The process of preparing the inner surface of the tube includes several steps. In each of these steps, the solutions necessary for the conditioning process are pumped into the borosilicate tube using a syringe and a flow rate of 10 $\mu L \cdot min^{-1}$ for one hour. The first step was to wash the inner wall of the tube using acetone to remove any organic matter, and then rinse with distilled water to remove any acetone residue. Then a sodium hydroxide 0.2 M solution was used to decompose the siloxane groups and increase the density of the silanol groups, then washed with distilled water to remove any remaining basic solution. Then, immediately after that, HCl acid with a concentration of 0.2M was used for the purpose of removing alkali metal ions.[10] The remainder was then washed with distilled water and ethanol. Finally, the borosilicate tube was injected with 3-trimethoxysilyl propyl methacrylate. Approximately an hour to allow for

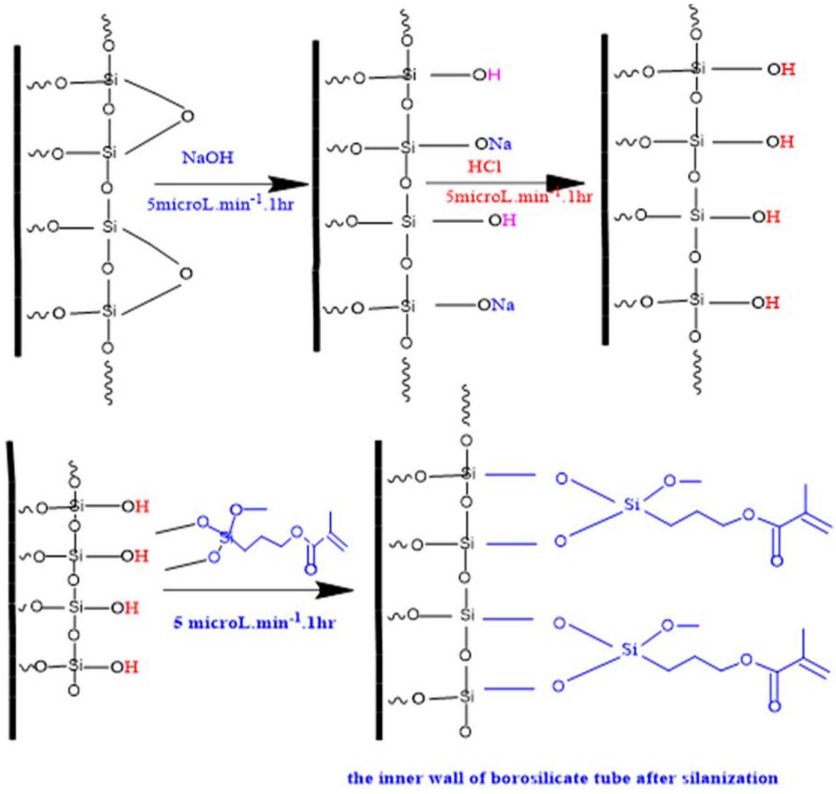

Fig. 2. Salinization process of borosilicate.[5]

reaction. N_2 gas was used to dry the tube. On the tube surface, silanol groups and trimethoxysilane groups are joined; the methacrylate groups will contribute to the polymerization reaction and the monolith to the glass tubes interior walls. The method used to prepare the inner surface of the column is similar to the preparation method described in reference.[5] *Fig.* 2, shown the Silanization process.

3. Result and Discussion

The polymerization process for the organic monolith was prepared through a mixture consisting of acrylic acid A.AC and glycidyl methacrylate GMA. GMA was chosen because it has two functional groups. The methacrylate double chain, which participates in the photopolymerization reaction, and the epoxy group. The presence of these functional groups makes GMA useful in many important chemical reactions and in modifying surfaces and polymers, rending it an important component in various Industries.[11]

Across-linker and progeny solvents were used, as well as an initiator, to start the reaction. The initiator 2,2-dimethoxy-2-phenylacetophenone DMAP was used instead of the initiator 2,2-azoisobutyronitrile AIBN, which is considered more commonly used but has several drawbacks. AIBN is considered dangerous due to its toxicity, potential for high-dose exposure, and long-term health problems. Additionally, it has limited thermal stability and is incompatible with certain monomers. Some monomers may not be compatible with the AIBN initiator due to their rapid reaction.[12]

The binding agent ethylene dimethacrylate EDMA is widely used in polymerization reactions, playing a crucial role in enhancing mechanical properties, controlling porosity, and facilitating the formation of stable polymers with large pore.[13] The percentage of the binder in the monomer significantly affects the porosity properties and chemical composition of the monolith column. For instance, increasing the percentage of the binder can result in higher polymerization density, which reduces pore size, enhances surface interactive forces, and improves separation efficiency. This, in turn, can impact the speed of material transfer and separation efficiency. Consequently, a monolith with a high surface area will exhibit limited permeability to solvents, leading to increased backpressure.[14] A binary solvent comprising ethanol and 1-hexanol was employed.

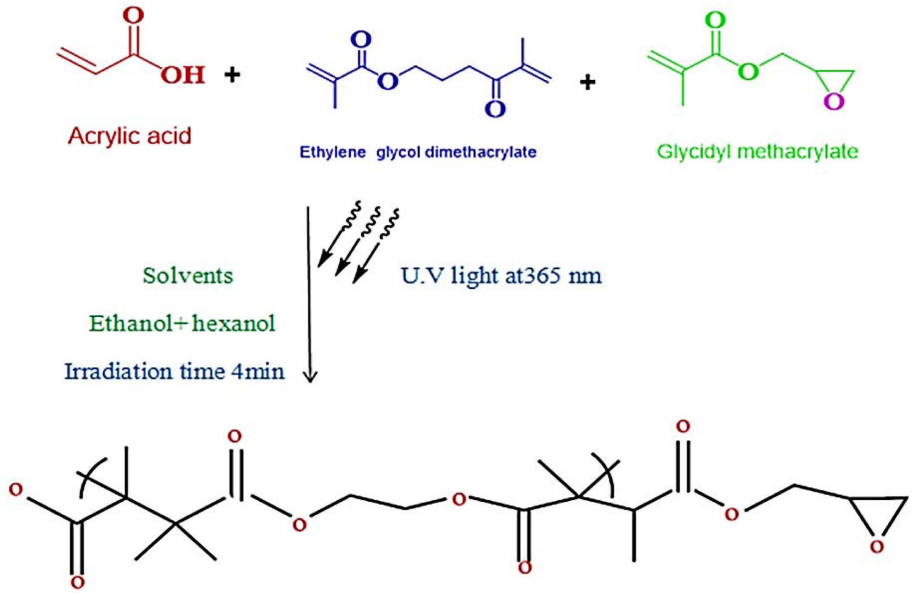

Fig. 3. The structure of monomers used in preparing monolith column.

The solvent plays a crucial in dissolving the monomers and the initiator, whereas it does not contribute to dissolving the polymer. The polymerization process was initiated using ultraviolet light (photopolymerization) with radicals. This method was chosen to form the monolith inside the tube due to its fast and efficient nature compared to traditional manufacturing processes, thereby reducing manufacturing time and increasing productivity. Ultraviolet rays offer high precision in formation and polymerization, enabling the production of intricate monolithic structures with more accuracy. Furthermore, adjustments in radiation intensity and exposure time provide precise control over the final properties of the monolith. Utilizing photopolymerization with ultraviolet radiation is considered a more economical and environmentally friendly process compared to some traditional methods involving harmful chemicals.[15] *Fig.* 3 illustrates the structure of monomers used to prepare the monolith.

3.1. Investigation of optimum condition of the polymer prepared

3.1.1. The effect of irradiation time

The optimal irradiation period for polymer synthesis was investigated after optimizing the monomer ratio distance between the irradiation source and the prepared column. The results were obtained using a variety of irradiation periods ranging from 1-6 minutes, and the results are shown according to *Table* 1. when no polymer formed inside the column: this result indicates a lack of polymerization, suggesting that the reaction did not occur or was incomplete. It provides objective data indicating the absence of polymer material within the column. And the polymer is not formed properly: this suggests that some polymerization occurrent, but it was insufficient or irregular. While not as definitive as the first result, it still provides objective data indicating suboptimal polymer formation, the polymer is formed by low back pressure: here, the formation of the polymer is indicated, accompanied by low pressure. This suggests that the polymerization process was successful to some extent, the polymer is formed by good back pressure: this result indicates successful polymer formation with optimal back pressure. It suggests that the polymerization process proceeded well, resulting in the formation of a polymer matrix within the column with desirable properties, the polymer is formed by high back pressure: this may imply a denser or more tightly cross-linked polymer structure compared to the previous result, the polymer is formed and very high back pressure: this result suggests that polymer formation occurred, but with excessive back pressure. This could indicate over-polymerization or the formation of a polymer matrix that is too dense, leading to increased resistance within the column.

Table 1. The effect of irradiation time on monolith formation

Irradiation	Result
1	No polymer is formed inside the column
2	The polymer is not formed properly
3	The polymer is formed by low back pressure
4	**The polymer is formed by good back pressure**
5	The polymer is formed by high back pressure
6	The polymer is formed and very high back pressure

3.1.2. Permeability and the porosity of the Monolith

Porosity refers to the empty spaces or voids within a material. It's a measure of how much of the material is empty, filled, with other substances. Porosity can be expressed as a percentage of the total volume of the material. Higher porosity and permeability generally mean there's more space for fluids to pass through. The porosity of the monolith was calculated by Eq. (1).

$$Ø = W_M - W_T / dL\, R^2 \pi \quad (1)$$

Porosity was calculated through the above equation and was equal to 0.096, where Ø = total porosity. W_M = weight of the monolith when filled with water: W_T = weight of the monolith when dried; d = density of water in 25 °C, d = 0.9965 g·cm^{-1}, L = monolith column length, R = cylindrical radius of the column; π = 3.14, the relationship between pressure and flow rate are related, as seen in *Fig.* 4.

3.1.3. Fourier-transform infrared spectroscopy FT-IR analysis

The FT-IR spectra of GMA-co-EDMA-co-A.AC

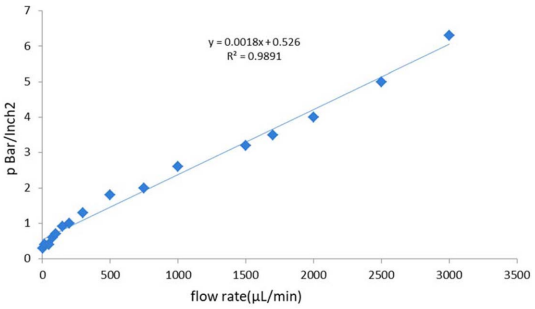

Fig. 4. The relationship between pressure and flow rate.

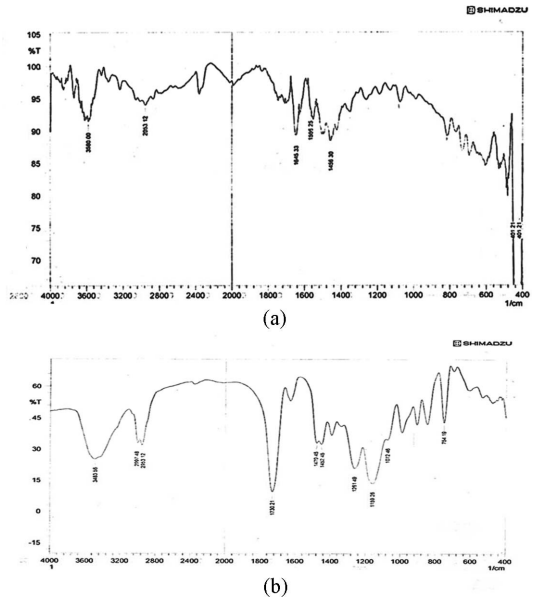

Fig. 5. (a) FT-IR spectra of GMA-co-EDMA-co-A.AC before epoxy group opening, (b) FT-IR spectra of GMA-co-EDMA-co-A.AC after epoxy group opening.

showed evidence of C=O, OH, and epoxy rings. When the C=C peaks in the cross-linker and monomer spectra disappear at the same time, Glycidyl methacrylate peaks around 850–1000 cm^{-1}, Ethylene dimethacrylate peaks around 1630–1725 cm^{-1} for C=O stretching of ester groups, acrylic acid peaks around 2900–310 cm^{-1} for OH stretching and peaks around 1700–1750 cm^{-1} for C=O stretching of carboxylic acid. This is clear evidence of polymer formation. *Fig.* 5(a) shows the FT-IR spectra of the prepared polymer. The polymer was created by a hydrolysis process utilizing a double syringe to injected hydrochloric acid for three hours at a flow rate of 10 $\mu L \cdot min^{-1}$ at a concentration of 0.2 M after the epoxy ring was opened. Hydroxyl groups OH are formed, this could manifest broad peaks around 3200–3600 cm^{-1} due to O-H stretching, change in Ester peaks the peaks corresponding to the ester groups from EDMA might shift slightly due to the change in the local environment caused by the reaction, Diol groups replaced the epoxy group, and *Fig.* 5(b) illustrates this translation. Whereas the epoxy group disappeared.

3.1.4. Scanning electron microscope SEM of the monolith GMA-co-EDMA-co-A.AC

The morphological properties of the monolith GMA-co-EDMA-co-A.AC have been investigated using SEM techniques. This is a technique used to examine the surface structure of a sample at very high magnification as shown in *Fig.* 6. It would involve studying the surface morphology, composition, and structure of the column material at a microscopic level.[16] the mobile phase was flowing through these pores readily, *Fig.* 4. Shown which is good for minimizing back pressure.

3.1.5. Brunauer-emmett-teller BET analysis of the monolith GMA-co-EDMA-co-A.AC

The Brunauer-Emmett-Teller BET method is a classical technique used to determine the specific area of porous materials by analysis gas adsorption isotherms, the results of BET analysis were 5.40 nm, 17.03 $m^2 \cdot g^{-1}$ of pore size and surface area, respectively; in this case, pore size and surface area are interrelated as pore size is needed for flow rate and surface area is required to provide a morphological environment to create reaction on the surface. The results are satisfactory, as high flow rates are obtained with moderate back pressure, and the reaction are carried out on the surface without hindrances.[17]

3.2. Method validation

3.2.1. Calibration curve

Each pharmaceutical substance, including warfarin, was assessed at wavelength of 326 nm as shown in *Fig.* 7. A calibration curve was constructed for warfarin with the range of 3-100 $\mu g \cdot mL^{-1}$, with a detection

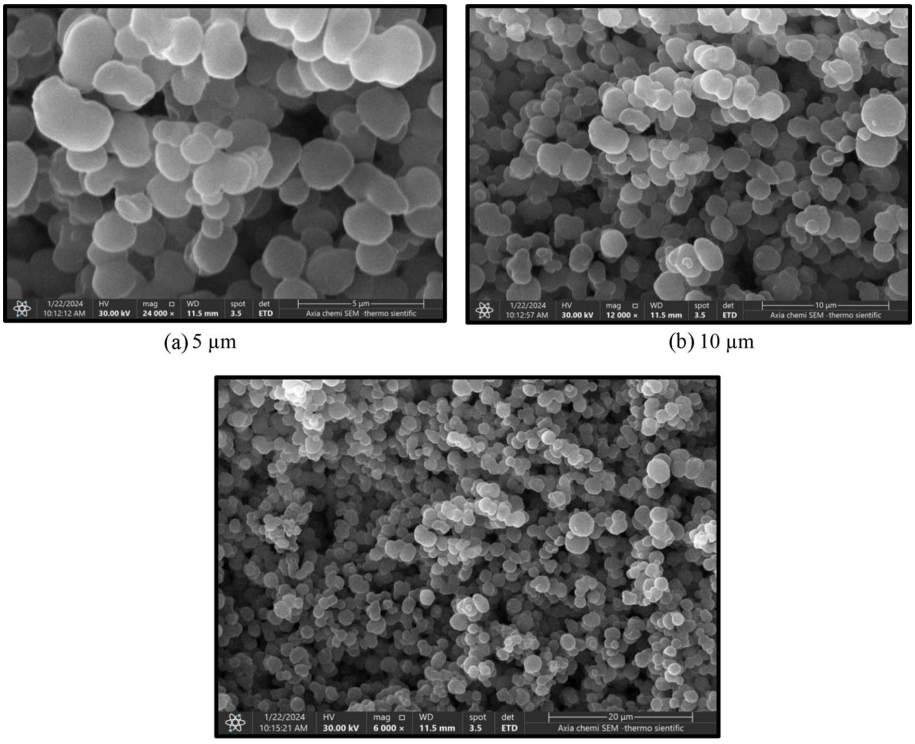

(a) 5 µm (b) 10 µm

(c) 20 µm

Fig. 6. (a, b, c) shows the SEM of the prepared monolith column GMA-co-EDMA-co-A.AC with different Magnification powers.

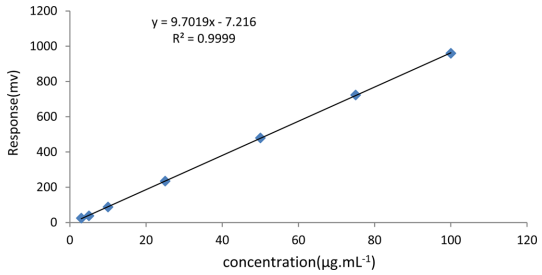

Fig. 7. Calibration curve of warfarin.

limit of 0.932 µg·mL^{-1} and a quantitative detection limit of 2.788 µg·mL^{-1}. *Table* 2 display the regression parameters.

3.2.2. Accuracy

The accuracy of the method was evaluated by determining the relative standard deviation RSD% during the day of the analysis n = 3 of the standard solution, selection three different concentrations from within the calibration curve 10, 25 and 50 µg·mL^{-1}.

Table 2. The analytical data of calibration curve of warfarin of the proposed method

Parameter	Suggested method
ε_{nm}	326
Concentration range µg·mL^{-1}	3-100
Slope	9.701
Determination coefficient r^2	0.999
Correlation coefficient r	0.999
Intercept	-7.216
D of slope	0.042
SD of intercept	2.227
LOD µg·mL^{-1}	0.932
LOQ µg·mL^{-1}	2.788
Sandell Sensitivity µg·cm^{-2}	103.1×10^{-3}
εL·mol^{-1}·cm^{-1}	2.99138×10^{6}

LOD: Limit of detection. LOQ: Limit of quantitation

The experiment was repeated three times, both within one day and over three consecutive days, and the results are displayed in *Table* 3. The intra-day precision for each concentration ranged from the intra-day

Table 3. Precession of the proposed method

Concentration μg·mL^{-1}	Intra-day precision Rec%	RSD%	Inter-day precision Rec%	RSD%
10	97.47	1.19	95.96	1.76
25	108.62	3.55	107.85	3.47
50	100.25	0.53	100.42	1.02

precision ranged from 0.53–3.55 %, while the inter-day precision ranged from 1.02–3.47 % The recovered amounts of the standard substance range from 95.26–100.48 % and the pharmaceutical compounds the range was from 62.10–87.69 %. This indicates the presence of interferences in determining the quantity of pharmaceuticals, as shown in *Table* 6.

3.2.3. Enrichment factor

Enrichment factor EF in the context of high-performance liquid chromatography HPLC is a measure of how much a particular compound is concentrated or enrichment in the sample compared to its concentration in the original concentration, it is often used in environment analysis, pharmaceutical analysis, and other field where trace compounds need to be detector and quantified accurately.[18] EF is defined as

EF = Ca/Cb, where Ca is the original concentration before enrichment, Cb is the initial concentration after enrichment, using the calibration curve equation y = 9.7019x–7.216, Ca = 960 ppm, Cb = 98.58 ppm, EF = 9.73.

Table 4. The evaluation results for monolith column

Pharmaceutical compounds	Theoretical value mg	Experimental value mg	RSD% N = 3
Warfarin	10	9.96	0.40

3.3. Application

The performance of the monolith column in determining the pharmaceutical compound was evaluated n = 3 by calculating the RSD% values using a prepared monolith connected to the Shimadzu 2010A system. The analysis was conducted under conditions of 90 % acetonitrile and 10 % water, with a flow rate of 0.3 mL·min^{-1}, as shown in *Table* 4. Additionally, the estimate amount of warfarin in commercial tablets containing 5 mg was effectively determined using the suggested approach; with outcomes in good agreement with the official USP standards. *Table* 5 indicates that there was no statistically significant different between the results produced using the official approach and the alternative method. Furthermore, the

Table 5. Statistical comparison of f-test and t-test data for HPLC monolith column with solid phase extraction by using U.V

t-test					
Technique	Variance.10^{-3}	t Calculated	t Tabled	P Probability	State
HPLC (monolith column) Solid phase extraction (UV)	5.233 18.143	2.452	2.776	0.035	Confidence
f-test					
Technique	Variance.10^{-3}	t Calculated	t Tabled	p Probability	State
HPLC (monolith column) Solid phase extraction (UV)	5.233 47.321	0.052	0.110	0.054	Confidence

Table 6. Determination of active substance of warfarin in different pharmaceutical preparations

Drug company	Concentration of active substance μg·mL^{-1} Present	Found	Rec%	SD	RSD%
Flamingo	10	6.23	62.32	0.16	22.88
Ciplato	50	40.53	87.69	0.26	5.92

Table 7. The most important methods used for the determination of warfarin

Technique	Stationary phase	Linear range µg. mL^{-1}	RSD%	Rec%	LOD µg·mL^{-1}	LOQ µg·mL^{-1}	Ref.
Normal Phase High Performance Liquid Chromatography	a Purospher STAR RP-18e (4 × 4 mm I.D. 5 m particle size)	0.1-6	>15	93.53	0.02	0.1	19
Continuous turbidimetric analysis	Solar cells with (37.8 mm (L) × 10 mm (W) × 1 mm, thickness	616.7-4934	1.95	_	0.57	_	20
Surface enhanced Raman scattering	20x (NA 0.4) LWD	3.7-11.1	6.71	102.04	0.56	1.77	21
An optoelectronic flow-through detector	_	0.9-154	2.59	_	0.79	2.59	22
Ultra violet	a Rheodyne 7000	0.0125-2.5	2.80	83.5	-	0.0125	23

active substance in warfarin was successfully estimated by the proposed method in pharmaceutical tablets, as shown in *Table* 7. The results of the proposed method were compared statistically with those obtained.

4. Conclusions

The homopolymer was successfully prepared inside a borosilicate tube using ultraviolet polymerization, achieving quick and cost-effective results. The ring-opening reaction of the Glycidyl methacrylate GMA epoxy group provided the monomer with ample opportunities to form and modify various groups on the surface of the homogeneous column. This versatility enabled the identification of pharmaceutical, ionic, and biological compounds using the technology. high-performance liquid chromatography HPLC was employed, and the pharmaceutical compound warfarin was effectively identified using a homogeneous column. The proposed method provides to be both fast and accurate, allowing for the determination of warfarin levels without the need for toxic chemicals. Furthermore, the procedures employed adhered to the principle of green chemistry, contributing to environmentally friendly practices. This method holds promise for quality control assessments, ensuring the integrity and efficacy of pharmaceutical products.

Acknowledgements

The authors thank the university and the Department of Chemistry for allowing them to use the laboratories and laboratory equipment.

References

1. S. Ražić, J. Arsenijević, S. Đogo Mračević, J. Mušović, and T. Trtić-Petrović, *Analyst*, **148**, 3130-3152 (2023). https://doi.org/10.1039/d3an00498h
2. H. Koh, W. Yau, P. Ong, and A. Hegde, *Drug. Discovery Today*, **8**, 889-897 (2023). https://doi:10.1016/S1359-6446(03)02846-0
3. S. Xie, R. Allington, J. Fréchet, and F. Svec, *Modern Advance in Chromatography*, **76**, 87-125 (2002). https://doi:10.1007/3-540-45345-8_3
4. N. Morales, S. Thickett, and F. Maya, *J. Sep. Sci.*, **46**, 18 (2023). https://doi:10.1002/jssc.202300378
5. N. S. Alsultani, A. A. Alkarimi, and I. A. Aljazaery, *J. Pharm. Negat. Results.*, **13**, 1629-1636 (2022). hptts://doi:10.47750/pnr.2022.13.04.226
6. J. Masini and F. Svec, *Anal. Chim. Acta*, **964**, 24-44 (2017). https://doi:10.1016/j.aca.2017.02.002
7. A. Sentkowska and K. Pyrzynska, *Molecules*, **26**, 5073 (2021). https://doi:10.3390/molecules26165073
8. L. Redón, X. Subirats, and M. Rosés. *Anal. Chim. Acta*, **1130**, 39-48 (2020). https://doi:10.1016/j.aca.2020.06.035
9. S. Treewaree, G. Y. H. Lip, and R. Krittayaphong, *Thromb. Haemost.*, **124**, 69-79 (2023). https://doi:10.1055/s-0043-1772773
10. J. J. Chruściel, *Polymers*, **14**, 4382 (2022). https://doi:10.3390/polym14204382
11. S. Alharthi and Z. El Rassi, *Molecules*, **25**, 1323 (2020). https://doi:10.3390/molecules25061323
12. R. Kardi, B. Etika, H. Sanjaya, and B. Oktavia, *Int. J. Sci. Res. Eng. Dev.*, **2**, 386-391 (2019).
13. P. Coufal, M. Čihák, J.Suchánková, E. Tesařová, Z. Bosáková, and K. Štulík, *J. Chromatogr. A,* **946**, 99-106

(2002). https://doi:10.1016/S0021-9673(01)01570-9
14. J. H. Kim, A. Y. Park, E. H. Jeong, C.-Y. Lee, T. H. Lee, and J. Youm, *Anal. Sci. Technol.*, **20**, 323-330 (2007).
15. S. Currivan and P. Jandera, *Chromatography,* **1**, 24-53 (2014). https://doi:10.3390/chromatography1010024
16. C. Aydoğan, B. Beltekin, N. Demir, B. Yurt, and Z. El Rassi, *Molecules*, **28**(3), 1423 (2023). https://doi:10.3390/molecules28031423
17. M. Tripathi, A. Bhatnagar, N. Mubarak, J. Sahu, and P. Ganesan, *Fuel*, **277**, 118184 (2020). https://doi:10.1016/j.fuel.2020.118184
18. R. Dolatabadi, A. Mohammadi, S. Nojavan, S. Yaripour, A. Tafakhori, and M. Shirangi, *J. Chinese Chem. Soc*., **68**(8), 1522-1530 (2021). https://doi:10.1002/jccs.202100016
19. Y. A. Chua, W. Z. Abdullah, Z. Yusof, and S. H. Gan, *ASM Sci. J*., **12**, 1-10 (2019). https://doi:10.32802/asmscj.2019.215
20. N. Turkey and J. Jeber, *J. Phys. Conf. Ser*., **2063**, 1-14 (2021). https://doi:10.1088/1742-6596/2063/1/012006
21. M. Sultan, M. Abou El-Alamin, A. Wark, and M. Azab, *Spectrochim. Acta - Part A Mol. Biomol. Spectrosc*., **228**, 117533 (2020). https://doi:10.1016/j.saa.2019.117533
22. J. N. Jeber and N. S. Turkey, *J. Pharm. Biomed. Anal*., **201**, 114128 (2021). https://doi:10.1016/j.jpba.2021.114128
23. P. Ring and J. Bostick. *J. Pharm. Biomed. Anal*., **22**(3), 573-581 (2000). https://doi:10.1016/S0731-7085(00)00232-6

Authors' Positions

Zahraa Hadi Shareef : Graduate Student
Ahmed Ali AL Karimi : Professor